International Journal of Computer Information Systems and Industrial Management Applications
ISSN 2150-7988 Volume 18(2s) 2026 pp. 59-80
https://doi.org/10.70917/ijcisim-2026-2065
Article

A MULTI-HYBRID DEEP LEARNING FRAMEWORK INTEGRATING TRANSFER LEARNING AND ENSEMBLE CLASSIFICATION FOR AUTOMATED PHOTOVOLTAIC PANEL DEFECT RECOGNITION

Priya Pal[1], Mukesh Yadav[2]

[1] Department of Electronics & Communication Engineering, SAGE University, Indore, India. Email: pal.priyaips@gmail.com
[2] Department of Electronics & Communication Engineering, SAGE University, Indore, India. Email: dr.mukesh71073@gmail.com
Corresponding Author: Priya Pal (Email: pal.priyaips@gmail.com)

Abstract: The rapid expansion of photovoltaic (PV) installations has increased the need for intelligent and automated defect detection systems capable of maintaining energy efficiency and operational reliability. Manual inspection of PV panels is time-consuming, labor-intensive, and prone to inaccuracies, particularly in large-scale solar farms. This study proposes a Multi-Hybrid Deep Learning Framework integrating transfer learning, deep feature extraction, and ensemble machine learning techniques for automated PV defect classification. Four models, namely PV-DenseFineNet, PV-DenseXGBHybridNet, PV-EfficientXGBHybridNet, and PV-MobileRFHybridNet, were developed using DenseNet121, EfficientNetV2B0, and MobileNetV3Large backbones combined with Softmax, XGBoost, and Random Forest classifiers. Experiments were conducted on a publicly available PV panel defect dataset containing six defect categories: Bird-drop, Clean, Dusty, Electrical-damage, Physical-damage, and Snow-covered. Comparative evaluation using Accuracy, Precision, Recall, F1-Score, ROC-AUC, and confusion matrix analysis demonstrated that PV-DenseFineNet achieved superior performance with 89.5% test accuracy and 0.987 ROC-AUC. The results confirm the effectiveness of end-to-end transfer learning for intelligent photovoltaic defect recognition and solar panel monitoring applications .

Keywords: Photovoltaic Defect Classification; Transfer Learning; DenseNet121; XGBoost; Deep Learning; Solar Panel Inspection.

1. Introduction

The growing demand for renewable energy has significantly accelerated the deployment of photovoltaic (PV) systems worldwide. Solar energy has emerged as one of the most sustainable and environmentally friendly energy sources, contributing substantially to global energy generation and carbon emission reduction initiatives. However, the long-term efficiency and reliability of photovoltaic installations are often affected by various defects, including dust accumulation, bird droppings, snow coverage, electrical faults, cracks, and physical damage. These defects reduce power generation efficiency, increase maintenance costs, and may eventually lead to severe system failures if not detected at an early stage.

Traditional PV inspection methods rely heavily on manual monitoring and periodic maintenance procedures. Such approaches are time-consuming, expensive, and difficult to scale for large solar farms. Recent advances in

computer vision and artificial intelligence have enabled automated fault diagnosis systems capable of detecting defects directly from solar panel images. Image-processing-based approaches have been applied for crack detection and fault identification in photovoltaic systems [1], [2], [4], [6]. More recently, deep learning methods, including convolutional neural networks (CNNs), YOLO-based object detectors, and EfficientNet architectures, have demonstrated promising results for photovoltaic defect recognition [3], [10], [11], [17], [18], [21], [25].

Despite these advancements, several challenges remain unresolved. First, many existing studies focus on a limited range of defect categories and fail to address multiple real-world PV faults simultaneously. Second, conventional CNN architectures often require large annotated datasets and extensive computational resources. Third, hybrid approaches integrating deep feature extraction with ensemble machine learning classifiers remain insufficiently explored for photovoltaic defect recognition. Furthermore, comparative investigations between end-to-end transfer learning models and hybrid machine learning frameworks are relatively scarce in the current literature.

To address these limitations, this study proposes a Multi-Hybrid Deep Learning Framework integrating transfer learning, deep feature extraction, and ensemble classification strategies for automated photovoltaic panel defect recognition. The framework employs three state-of-the-art CNN backbones, namely DenseNet121, EfficientNetV2B0, and MobileNetV3Large, to extract discriminative feature representations from PV images. These features are subsequently classified using Softmax, XGBoost, and Random Forest classifiers to investigate the effectiveness of different hybrid learning strategies.

The primary contributions of this research are summarized as follows:

Development of a novel multi-hybrid framework integrating transfer learning and ensemble machine learning for photovoltaic defect classification.

Design and implementation of four classification models: PV-DenseFineNet, PV-DenseXGBHybridNet, PV-EfficientXGBHybridNet, and PV-MobileRFHybridNet.

Comprehensive evaluation on a publicly available PV defect dataset containing six defect categories.

Comparative analysis of end-to-end CNN learning and feature-based ensemble learning approaches.

Identification of the most effective architecture for intelligent solar panel monitoring systems.

The remainder of this paper is organized as follows. Section 2 presents a comprehensive literature review of existing photovoltaic defect detection and classification techniques. Section 3 describes the proposed multi-hybrid deep learning framework, including preprocessing, feature extraction, and classification methodologies. Section 4 discusses implementation details, dataset characteristics, and experimental settings. Section 5 presents performance evaluation and comparative result analysis. Finally, Section 6 concludes the study and outlines future research directions.

2. Literature Review

Automated photovoltaic (PV) defect detection has attracted considerable attention due to the growing deployment of solar energy systems and the increasing need for intelligent maintenance solutions. Early studies primarily relied on image processing techniques to identify cracks and surface defects in solar panels. Feng et al. [2] proposed a crack detection algorithm based on image analysis techniques, demonstrating the feasibility of automated PV inspection. Similarly, Aghamohammadi et al. [6] employed Particle Swarm Optimization for solar panel crack detection, while Yao and Wu [4] developed a Halcon-based vision framework for identifying surface defects. Song et al. [14] further improved crack detection performance using multi-scale image processing and region-growing techniques.

With the advancement of machine learning technologies, researchers began integrating classification algorithms into photovoltaic fault diagnosis systems. Padmavathi and Chilambuchelvan [13] introduced a fault identification system utilizing communication technologies for monitoring solar panel conditions. Shanthosh et al. [16] combined image processing and IoT technologies to create intelligent solar fault identification frameworks. These studies demonstrated the potential of automated monitoring but remained dependent on handcrafted feature engineering techniques.

Deep learning has recently emerged as the dominant paradigm for photovoltaic defect recognition. Convolutional Neural Networks (CNNs) automatically learn hierarchical feature representations from images and significantly outperform conventional machine learning methods. Pa et al. [12] developed a CNN-based photovoltaic

fault detection framework achieving high classification accuracy. Vallampalli et al. [10] proposed a web-based CNN system for solar panel defect detection and classification, highlighting the practical applicability of deep learning in real-world environments. Mahmud et al. [18] evaluated VGG16 and VGG19 architectures for solar panel fault diagnosis and reported strong classification performance across multiple defect categories.

Recent studies have focused on improving defect detection accuracy through advanced deep learning architectures and object detection frameworks. Wang et al. [3] utilized the YOLOv8 algorithm for photovoltaic crack recognition and demonstrated effective localization performance. Moghadam et al. [11] proposed UAV-assisted solar panel inspection using YOLO-based models, enabling large-scale defect monitoring. Wong and Phang [20] investigated enhancements to YOLO architectures for RGB-image-based solar panel fault detection, reporting improved detection capability under challenging conditions.

Transfer learning has become particularly attractive for photovoltaic defect classification because it reduces training requirements and improves generalization. Joshua et al. [21] employed EfficientNetB0 for AI-powered solar panel maintenance and fault detection, demonstrating the effectiveness of pretrained deep learning models. Manimegalai et al. [17] integrated GAN and EfficientNet architectures to improve defect recognition performance, while Safaei et al. [19] proposed a semi-supervised learning framework to address limited labeled data availability. These studies confirm that transfer learning can significantly enhance photovoltaic inspection performance.

Ensemble learning techniques have also been explored to improve classification robustness. Jayapriya and Kalaivani [5] proposed a hybrid CNN-SVM model for efficient crack and fault detection, achieving improved classification accuracy compared with standalone CNN models. Jana et al. [7] introduced CrackSense, an ensemble-learning-based solar panel inspection framework capable of improving detection reliability. Similarly, Boutana et al. [15] employed multi-modal fault detection models to enhance photovoltaic diagnosis performance. These studies suggest that combining deep feature extraction with machine learning classifiers can improve predictive capability under specific conditions.

Research has also investigated environmental contamination defects such as dust accumulation and surface degradation. Karima et al. [8] developed an image-processing-based dust detection system capable of identifying contamination levels on photovoltaic panels. Xia et al. [24] proposed a defect recognition framework based on percolation-driven image processing methods and demonstrated effective surface defect analysis. Reji and Maxwell [9] employed electroluminescence imaging combined with computer vision techniques for microcrack detection, providing highly detailed structural analysis of photovoltaic cells.

More recently, advanced deep learning architectures have been proposed for intelligent photovoltaic monitoring systems. Rohith et al. [25] introduced SparkNet, a deep learning model specifically designed for solar panel fault detection. K. N. et al. [1] combined crack detection and power output analysis to establish a comprehensive photovoltaic maintenance framework. Ramya et al. [22] utilized VGG-based architectures for defect detection and performance analysis, further demonstrating the applicability of transfer learning approaches.

Although significant progress has been achieved, several research gaps remain. Most existing studies focus on either end-to-end CNN learning or conventional machine learning classifiers independently. Comparative investigations involving multiple transfer learning architectures integrated with ensemble classifiers are limited. Furthermore, the relative effectiveness of deep feature extraction combined with XGBoost and Random Forest classifiers remains insufficiently explored for multiclass photovoltaic defect recognition. Motivated by these limitations, the present study develops a comprehensive Multi-Hybrid Deep Learning Framework integrating DenseNet121, EfficientNetV2B0, MobileNetV3Large, XGBoost, Random Forest, and Softmax classification strategies. The proposed framework provides a systematic comparison of transfer learning and ensemble learning approaches for intelligent photovoltaic defect classification and contributes toward the development of robust solar panel monitoring systems.

3. Proposed Methodology

The proposed framework introduces a **Multi-Hybrid Deep Learning Architecture for Photovoltaic (PV) Panel Defect Classification**, integrating transfer learning, deep feature extraction, and ensemble machine learning classifiers. The architecture employs three state-of-the-art convolutional neural network (CNN) backbones—DenseNet121, EfficientNetV2B0, and MobileNetV3Large—to learn discriminative defect representations from solar panel images. Subsequently, extracted deep features are classified using Softmax, XGBoost, and Random Forest classifiers to enhance defect recognition performance.

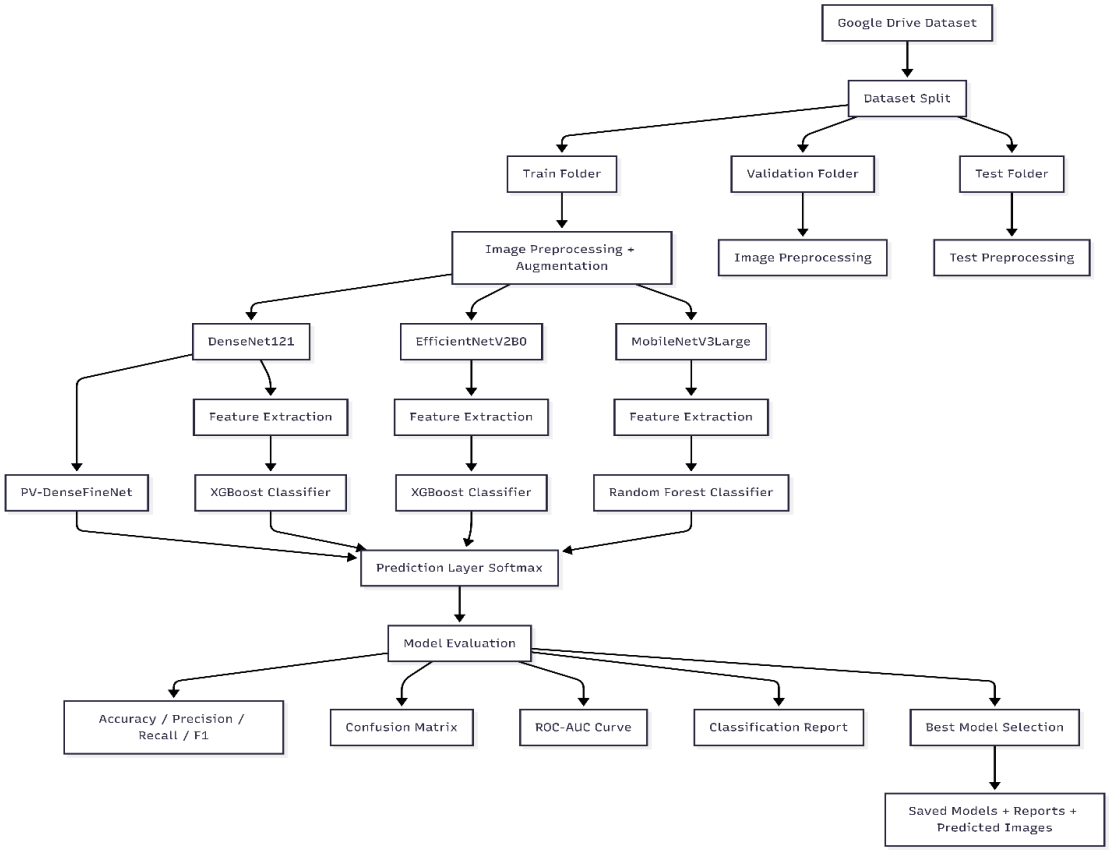

Figure 1. Proposed Multi-Hybrid Deep Learning Framework for Photovoltaic Panel Defect Classification

Figure 1 illustrates the overall architecture of the proposed Multi-Hybrid Deep Learning Framework developed for photovoltaic (PV) panel defect classification. The framework begins with the acquisition of PV panel images from a Google Drive dataset repository, followed by dataset partitioning into training, validation, and testing subsets. During preprocessing, image normalization and augmentation techniques are applied to improve data quality and enhance model generalization. Three transfer learning backbones, namely DenseNet121, EfficientNetV2B0, and MobileNetV3Large, are employed to extract discriminative deep feature representations from the input images. The extracted features are subsequently processed through different classification strategies, including the proposed PV-DenseFineNet, XGBoost-based hybrid models, and a Random Forest-based hybrid model. The outputs from these classifiers are integrated through a prediction layer to generate final defect predictions. Model performance is then evaluated using standard metrics such as Accuracy, Precision, Recall, F1-Score, Confusion Matrix, ROC-AUC Curve, and Classification Report. Finally, the best-performing model is selected and stored along with trained weights, evaluation reports, and predicted images for future deployment in intelligent solar panel inspection and monitoring systems. This architecture provides a comprehensive end-to-end framework for automated photovoltaic defect detection, classification, and performance assessment.

3.1 Dataset Acquisition and Partitioning

The PV image dataset is collected from a Google Drive repository and organized into training, validation, and testing subsets.

Let the complete dataset be represented as:

$$D = \{(x_i, y_i)\}_{i=1}^{N} \quad (1)$$

where:

$x_i$denotes the i^{th}PV panel image.

$y_i$represents the corresponding defect class label.

$N$is the total number of images.

The dataset is partitioned into:

$$D = D_{train} \cup D_{val} \cup D_{test} \quad (2)$$

subject to

$$D_{train} \cap D_{val} \cap D_{test} = \emptyset \quad (3)$$

where:

D_{train}= Training dataset

D_{val}= Validation dataset

D_{test}= Testing dataset

3.2 Image Preprocessing and Augmentation

Each image is resized to a fixed resolution of 256×256pixels.

The resized image is expressed as:

$$I_r = Resize(I, 256{,}256) \quad (4)$$

where:

I= Original image

I_r= Resized image

Normalization

Pixel intensities are normalized into the range $[0, 1]$:

$$I_n = \frac{I_r}{255} \quad (5)$$

where:

I_n= Normalized image

Data Augmentation

Random transformations are applied to improve generalization:

$$I_a = T(I_n) \quad (6)$$

where $T(\cdot)$represents:

Rotation

Zooming

Translation

Horizontal flipping

Brightness adjustment

The augmented image is then forwarded to the feature extraction stage.

3.3 Deep Feature Extraction using Transfer Learning

Three pretrained CNN architectures are employed:

DenseNet121

EfficientNetV2B0

MobileNetV3Large

Given an input image I_a, feature extraction is defined as:

$$F = \phi(I_a) \qquad (7)$$

where:

F= Deep feature representation

$\phi(\cdot)$= CNN backbone function

3.3.1 DenseNet121 Feature Learning

DenseNet establishes direct connectivity between all preceding layers.

The feature propagation can be expressed as:

$$x_l = H_l([x_0, x_1, \dots, x_{l-1}]) \qquad (8)$$

where:

x_l= Output of layer l

$H_l(\cdot)$= Composite operation

$[\ \cdot\ ]$= Feature concatenation

This structure promotes feature reuse and alleviates vanishing gradients.

3.3.2 EfficientNetV2B0 Feature Learning

EfficientNet scales network dimensions uniformly.

The compound scaling relationship is:

$$Depth = \alpha^{\phi} \qquad (9)$$
$$Width = \beta^{\phi} \qquad (10)$$
$$Resolution = \gamma^{\phi} \qquad (11)$$

subject to

$$\alpha\beta^2\gamma^2 \approx 2 \qquad (12)$$

where:

ϕ= Scaling coefficient

α, β, γ= Scaling constants

3.3.3 MobileNetV3 Feature Learning

MobileNetV3 utilizes depthwise separable convolution.

The computational complexity becomes:

$$Cost_{DW} = D_k^2 M D_f^2 + M N D_f^2 \qquad (13)$$

where:

D_k= Kernel size

M= Input channels

N= Output channels

D_f= Feature map size

This significantly reduces computational overhead.

3.4 Global Average Pooling and Feature Vector Generation

Feature maps generated by CNN backbones are converted into compact feature vectors using Global Average Pooling (GAP).

$$f_j = \frac{1}{HW} \sum_{h=1}^{H} \sum_{w=1}^{W} A_j\,(h, w) \qquad (14)$$

where:

A_j= Activation map

H, W= Spatial dimensions

The final feature vector becomes:

$$F = [f_1, f_2, \ldots, f_k] \qquad (15)$$

where $k$denotes the feature dimension.

3.5 Hybrid Classification Framework

The proposed framework employs three hybrid classification mechanisms.

3.5.1 PV-DenseFineNet (CNN Softmax)

The DenseNet classifier predicts class probabilities through Softmax activation:

$$P(y = i \mid x) = \frac{e^{z_i}}{\sum_{j=1}^{C} e^{z_j}} \qquad (16)$$

where:

z_i= Logit score

C= Number of defect classes

The predicted label is:

$$\hat{y} = \arg\max_i P(y = i \mid x) \qquad (17)$$

3.5.2 DenseNet121 + XGBoost Hybrid

The extracted feature vector $F$is supplied to XGBoost.

The ensemble prediction is:

$$\hat{y} = \sum_{k=1}^{K} f_k\,(F) \qquad (18)$$

where:

f_k= Decision tree

K= Total trees

The objective function is:

$$Obj = \sum_{i=1}^{n} l(\,y_i, \hat{y}_i) + \sum_{k=1}^{K} \Omega(\,f_k) \qquad (19)$$

where:

$l(\cdot)$= Loss function

$\Omega(\cdot)$= Regularization term

3.5.3 EfficientNetV2B0 + XGBoost Hybrid

The same deep feature representation generated by EfficientNetV2B0 is processed using XGBoost.

$$F_{Eff} = \phi_{Eff}(I_a) \quad (20)$$
$$\hat{y}_{Eff} = XGB(F_{Eff}) \quad (21)$$

3.5.4 MobileNetV3 + Random Forest Hybrid

Feature vectors are classified using Random Forest.

The final decision is obtained by majority voting:

$$\hat{y} = mode(T_1(F), T_2(F), \dots, T_n(F)) \quad (22)$$

where:

T_i= Individual decision tree

n= Number of trees

3.6 Model Evaluation

The performance of each model is evaluated using standard classification metrics.

Accuracy

$$Accuracy = \frac{TP + TN}{TP + TN + FP + FN} \quad (23)$$

where:

TP = True Positive

TN = True Negative

FP = False Positive

FN = False Negative

Precision

$$Precision = \frac{TP}{TP + FP} \quad (24)$$

Recall

$$Recall = \frac{TP}{TP + FN} \quad (25)$$

F1-Score

$$F1 = 2 \times \frac{Precision \times Recall}{Precision + Recall} \quad (26)$$

ROC Curve

The true positive rate is:

$$TPR = \frac{TP}{TP + FN} \quad (27)$$

The false positive rate is:

$$FPR = \frac{FP}{FP + TN} \qquad (28)$$

The area under the ROC curve is computed as:

$$AUC = \int_0^1 TPR(FPR)\, d(FPR) \qquad (29)$$

3.7 Best Model Selection

The optimal model is selected based on maximum testing accuracy.

$$M^* = \arg\max_m (Accuracy_m) \qquad (30)$$

where:

M^*= Best-performing model

$Accuracy_m$= Accuracy of model m

The selected model is stored together with confusion matrices, ROC curves, classification reports, trained weights, and predicted defect images for deployment in intelligent solar farm monitoring systems.

3.8 Proposed algorithm

Algorithm 1: Dataset Preparation and Image Preprocessing

The first stage of the proposed framework focuses on dataset acquisition, partitioning, image preprocessing, and augmentation. Initially, the photovoltaic (PV) image dataset is loaded from the Google Drive repository and mathematically represented using Equation (1). Subsequently, the dataset is divided into training, validation, and testing subsets according to Equation (2), while ensuring mutual exclusivity among the subsets as defined in Equation (3). Each image is resized to a fixed resolution of 256×256 pixels using Equation (4) and normalized using Equation (5) to standardize pixel intensity values. To improve model generalization and reduce overfitting, data augmentation operations such as rotation, zooming, brightness adjustment, and horizontal flipping are applied using Equation (6). The resulting preprocessed datasets are then forwarded to the feature extraction stage.

Algorithm 1: Dataset Preparation and Image Preprocessing

Input: PV Image Dataset D

Output: Preprocessed Training, Validation and Testing Sets

Load PV image dataset from Google Drive repository.

Represent the dataset using Equation (1).

Split the dataset into training, validation and testing sets using Equation (2).

Ensure data exclusivity according to Equation (3).

For each image:

Resize image using Equation (4).

Normalize image using Equation (5).

Apply augmentation on training images using Equation (6).

Generate augmented samples.

Create train, validation and test generators.

Return preprocessed datasets.

Algorithm 2: CNN-Based Deep Feature Extraction

The second stage aims to extract highly discriminative representations from photovoltaic panel images using transfer learning. Three pretrained deep learning architectures, namely DenseNet121, EfficientNetV2B0, and MobileNetV3Large, are employed as feature extraction backbones. For each input image, deep features are generated according to Equation (7). DenseNet121 performs feature propagation through dense connectivity as defined by Equation (8), whereas EfficientNetV2B0 utilizes compound scaling represented by Equations (9)–(12). MobileNetV3Large employs depthwise separable convolution to reduce computational complexity according to Equation (13). The extracted feature maps are transformed into compact feature vectors through global average pooling using Equation (14), and the final feature representation is generated according to Equation (15). These feature vectors are stored for subsequent hybrid classification.

Algorithm 2: CNN-Based Deep Feature Extraction

Input: Preprocessed Images

Output: Deep Feature Vectors

Initialize DenseNet121, EfficientNetV2B0 and MobileNetV3Large.

Load pretrained ImageNet weights.

Remove the original classification layers.

Freeze initial convolutional layers.

For each preprocessed image:

Extract deep features using Equation (7).

Perform DenseNet feature propagation using Equation (8).

Apply EfficientNet scaling using Equations (9)–(12).

Apply MobileNet depthwise convolution using Equation (13).

Perform global average pooling using Equation (14).

Generate feature vector using Equation (15).

Store extracted feature vectors.

Return feature repository.

Algorithm 3: Multi-Hybrid Model Training and Classification

The third stage performs hybrid classification using deep features extracted from the CNN backbones. Four classification models are developed, namely PV-DenseFineNet, PV-DenseXGBHybridNet, PV-EfficientXGBHybridNet, and PV-MobileRFHybridNet. In PV-DenseFineNet, DenseNet121 features are classified using the Softmax function represented by Equation (16), and the final class label is determined using Equation (17). For PV-DenseXGBHybridNet, DenseNet features are supplied to the XGBoost classifier, where ensemble prediction and objective optimization are performed using Equations (18) and (19), respectively. Similarly, EfficientNetV2B0 features are classified through XGBoost using Equations (20) and (21). MobileNetV3Large features are processed through a Random Forest classifier, and final decisions are obtained through majority voting according to Equation (22). The trained models are then stored for evaluation.

Algorithm 3: Multi-Hybrid Model Training and Classification

Input: Deep Feature Vectors and Class Labels

Output: Trained Hybrid Classification Models

Initialize four classification models.

Train PV-DenseFineNet:

Compute Softmax probabilities using Equation (16).

Generate class prediction using Equation (17).

Train PV-DenseXGBHybridNet:

Apply XGBoost ensemble prediction using Equation (18).

Optimize objective function using Equation (19).

Train PV-EfficientXGBHybridNet:

Generate EfficientNet feature representation using Equation (20).

Perform XGBoost classification using Equation (21).

Train PV-MobileRFHybridNet:

Apply Random Forest voting mechanism using Equation (22).

Save trained models and learned parameters.

Return trained hybrid models.

Algorithm 4: Performance Evaluation and Best Model Selection

The final stage evaluates the performance of all trained hybrid models using standard classification metrics. Each model predicts defect classes for the testing dataset, and performance measures are computed. Accuracy, precision, recall, and F1-score are calculated using Equations (23)–(26), respectively. Furthermore, the true positive rate and false positive rate are computed using Equations (27) and (28), while the area under the ROC curve is determined using Equation (29). Confusion matrices and classification reports are generated to analyze class-wise prediction performance. Finally, the best-performing model is selected based on the maximum testing accuracy according to Equation (30). The selected model, along with all reports and visualization outputs, is stored for future deployment in intelligent solar monitoring systems.

Algorithm 4: Performance Evaluation and Best Model Selection

Input: Trained Hybrid Models and Testing Dataset

Output: Best Performing Model

Load trained models.

For each model:

Predict test class labels.

Compute Accuracy using Equation (23).

Compute Precision using Equation (24).

Compute Recall using Equation (25).

Compute F1-Score using Equation (26).

Compute True Positive Rate using Equation (27).

Compute False Positive Rate using Equation (28).

Compute ROC-AUC using Equation (29).

Generate confusion matrix.

Generate classification report.

Store all evaluation results.

Select the optimal model using Equation (30).

Save:

Best model weights.

ROC curves.

Confusion matrices.

Classification reports.

Predicted defect images.

Return the final best-performing model.

3.9 Comparison of Proposed Hybrid Deep Learning Models

To comprehensively investigate the effectiveness of different deep feature extraction and classification strategies for photovoltaic (PV) panel defect recognition, four proposed models are developed and evaluated. The models differ in terms of backbone architecture, feature extraction capability, classifier design, computational complexity, and generalization performance. DenseNet121 is selected due to its dense connectivity mechanism that promotes feature reuse and alleviates gradient degradation. EfficientNetV2B0 is incorporated because of its compound scaling strategy, which provides an excellent trade-off between accuracy and computational efficiency. MobileNetV3Large is utilized to enable lightweight deployment in resource-constrained edge environments. Furthermore, XGBoost and Random Forest classifiers are integrated with deep feature representations to exploit the advantages of ensemble learning and improve decision boundaries beyond conventional Softmax classification.

The hyperparameter settings are carefully selected through empirical experimentation and validation performance analysis. The objective is to ensure fair comparison among all proposed models while maintaining robust classification performance for multiple PV defect categories.

Table 1 Comparison of Proposed Models, Features, Justification, and Hyperparameters

Model Name	Backbone Network	Classification Method	Key Features	Justification	Major Hyperparameters
PV-DenseFineNet	DenseNet121	Softmax Classifier	Dense connectivity, feature reuse, transfer learning, end-to-end optimization	DenseNet121 effectively propagates low-level and high-level defect information through dense feature connections, improving defect localization and classification accuracy while reducing vanishing gradient problems.	Learning Rate = 1e-4 (Head Training), Fine-Tuning LR = 3e-6, Epochs = 80, Batch Size = 8, Dropout = 0.30, Dense Units = 512, Freeze Layers = 140

PV-DenseXGBHybridNet	DenseNet121	XGBoost	Deep feature extraction + Gradient Boosting Ensemble	DenseNet121 generates highly discriminative feature vectors, while XGBoost improves classification robustness through sequential boosting and regularized tree optimization, making it suitable for complex defect patterns.	XGBoost Estimators = 500, Learning Rate = 0.02, Max Depth = 4, Subsample = 0.90, Colsample = 0.90, Freeze Layers = 140
PV-EfficientXGBHybridNet	EfficientNetV2B0	XGBoost	Compound-scaled feature learning, parameter-efficient architecture, boosted classification	EfficientNetV2B0 provides strong feature representation with fewer parameters and lower computational cost. Combining it with XGBoost enhances non-linear decision-making capability and improves generalization on unseen defect samples.	XGBoost Estimators = 500, Learning Rate = 0.02, Max Depth = 4, Subsample = 0.90, Colsample = 0.90, Freeze Layers = 180
PV-MobileRFHybridNet	MobileNetV3Large	Random Forest	Lightweight CNN, depthwise separable convolution, ensemble tree voting	MobileNetV3Large is optimized for edge deployment and low computational overhead. Random Forest enhances robustness through multiple decision trees and majority voting, reducing prediction variance and overfitting.	Random Forest Trees = 500, Max Depth = None, Class Weight = Balanced, Batch Size = 8, Freeze Layers = 180

Table 2. Feature-Level Comparative Analysis

Feature Category	PV-DenseFineNet	PV-DenseXGBHybridNet	PV-EfficientXGBHybridNet	PV-MobileRFHybridNet
Transfer Learning	✓	✓	✓	✓
End-to-End CNN Learning	✓	✗	✗	✗
Deep Feature Extraction	✓	✓	✓	✓
Ensemble Learning	✗	✓	✓	✓
Gradient Boosting	✗	✓	✓	✗
Random Forest Voting	✗	✗	✗	✓
Computational Efficiency	Medium	Medium	High	Very High
Feature Reuse Capability	Very High	Very High	High	Medium
Edge Deployment Suitability	Medium	Medium	High	Very High
Expected Generalization Ability	High	Very High	Very High	High
Model Complexity	High	High	Medium	Low

Among the proposed architectures, **PV-DenseFineNet** serves as the baseline deep learning model by performing direct Softmax classification on DenseNet121 features. **PV-DenseXGBHybridNet** extends this framework by replacing the final neural classifier with XGBoost, allowing boosted decision trees to learn complex defect boundaries from deep representations. **PV-EfficientXGBHybridNet** focuses on achieving a balance between computational efficiency and predictive performance by combining EfficientNetV2B0 with XGBoost. Finally, **PV-MobileRFHybridNet** targets lightweight deployment scenarios, where MobileNetV3Large generates compact features that are classified using a Random Forest ensemble. Consequently, the four proposed models collectively provide a comprehensive comparison between conventional CNN classification, gradient boosting-based hybrid learning, and lightweight ensemble-based defect recognition approaches for intelligent photovoltaic monitoring systems.

4. Implementation

4.1 Hardware and Software Environment

The proposed Multi-Hybrid Deep Learning Framework was implemented using Python-based machine learning and deep learning libraries within the Google Colaboratory environment. The experimental setup combines transfer learning, feature extraction, and ensemble learning techniques to classify photovoltaic (PV) panel defects. All experiments were conducted using TensorFlow/Keras for deep neural network training, Scikit-learn for machine learning operations, XGBoost for gradient boosting classification, and Pandas/NumPy for data manipulation and

preprocessing. The trained models, generated reports, confusion matrices, ROC curves, and prediction outputs were stored in Google Drive for persistent storage and reproducibility.

Table 3 Hardware Configuration

Component	Specification
Computing Platform	Google Colaboratory
Processor	Intel Xeon CPU (Cloud Environment)
GPU	NVIDIA Tesla T4 / A100 (Subject to Availability)
RAM	12–25 GB
Storage	Google Drive Cloud Storage
Runtime Environment	Linux-based Cloud Instance
Internet Connectivity	High-Speed Cloud Network

Table 4 Software Configuration

Software Component	Version/Description
Operating Environment	Google Colab Linux Runtime
Programming Language	Python 3.x
Deep Learning Framework	TensorFlow 2.x
Neural Network API	Keras
Machine Learning Library	Scikit-Learn
Gradient Boosting Library	XGBoost
Data Analysis Library	Pandas
Numerical Computing	NumPy
Visualization Tools	Matplotlib, Seaborn
Image Processing	Pillow (PIL)
Model Serialization	Joblib
Spreadsheet Support	OpenPyXL

4.2 Dataset Description

The photovoltaic panel defect dataset utilized in this study was obtained from the publicly available Kaggle repository entitled **"PV Panel Defect Dataset"** developed by Alicja Lenarczyk. The dataset was specifically designed for photovoltaic defect classification research and contains labeled solar panel images belonging to multiple defect categories. The dataset integrates images collected from publicly available sources and provides a structured benchmark for evaluating machine learning, transfer learning, and hybrid deep learning approaches for automatic photovoltaic fault diagnosis.

The dataset contains six defect classes representing common photovoltaic panel conditions encountered in real-world solar energy systems. These classes include bird-dropping contamination, dust accumulation, electrical damage, physical damage, snow coverage, and defect-free clean panels. Such categories enable comprehensive evaluation of intelligent inspection systems under diverse environmental and operational conditions.

Table 5 PV Panel Defect Classes

Class Label	Description
Bird-drop	PV panels contaminated with bird droppings
Clean	Defect-free photovoltaic panels operating under normal conditions
Dusty	Panels covered by dust accumulation
Electrical-damage	Hotspots, delamination, electrical faults, and cell degradation
Physical-damage	Cracks, broken glass, and mechanical defects
Snow-covered	Panels partially or fully covered by snow

The dataset contains a total of **1,574 photovoltaic images** distributed across training, validation, and testing subsets. The dataset was intentionally curated to maintain a relatively balanced distribution among classes, thereby reducing classification bias and improving model generalization.

Table 6 Dataset Distribution

Class	Training	Validation	Testing	Total
Bird-drop	177	104	17	298
Clean	169	102	18	289
Dusty	162	97	16	275
Electrical-damage	135	77	13	225
Physical-damage	132	78	15	225
Snow-covered	154	92	16	262
Total	**929**	**550**	**95**	**1574**

The dataset structure follows a directory-based organization consisting of separate training, validation, and testing folders. Each folder contains six subdirectories corresponding to the defect categories. This arrangement enables seamless integration with TensorFlow ImageDataGenerator and transfer learning pipelines.

Table 7 Dataset Organization

Dataset Split	Purpose
Train	Model learning and parameter optimization
Validation	Hyperparameter tuning and overfitting monitoring
Test	Final performance evaluation and benchmarking

Prior to model training, all images were resized to a resolution of **256 × 256 pixels** and normalized according to the preprocessing requirements of the corresponding CNN backbone architecture. Data augmentation techniques, including rotation, zooming, brightness adjustment, width shifting, height shifting, and horizontal flipping, were applied exclusively to the training set to enhance data diversity and improve generalization performance. These preprocessing operations help the proposed models learn robust defect representations under varying environmental and imaging conditions.

The balanced nature of the dataset, combined with its diverse defect categories, makes it particularly suitable for evaluating the proposed hybrid architectures, namely PV-DenseFineNet, PV-DenseXGBHybridNet, PV-EfficientXGBHybridNet, and PV-MobileRFHybridNet. Furthermore, the dataset provides an effective benchmark for assessing transfer learning, deep feature extraction, ensemble learning, and automated photovoltaic inspection systems.

Dataset source :

Lenarczyk, A. *PV Panel Defect Dataset*. Kaggle Repository. Available at:

https://www.kaggle.com/datasets/alicjalena/pv-panel-defect-dataset

4.3 Illustrative Analysis

Figure 2. Sample Prediction Results of the Proposed Hybrid PV Defect Classification Framework

Figure 2 presents representative photovoltaic panel images selected from the testing dataset along with their corresponding predicted labels generated by the proposed hybrid defect classification framework. The figure illustrates successful identification of multiple defect categories, including **Dusty** and **Snow-Covered** panels. For each image, the actual class label, predicted class label, confidence score, and image source location are displayed. The results demonstrate the capability of the proposed model to recognize environmental contamination and weather-related defects under diverse operating conditions. Furthermore, the confidence scores provide additional insight into the model's prediction certainty and decision-making behavior when classifying real-world PV panel defects.

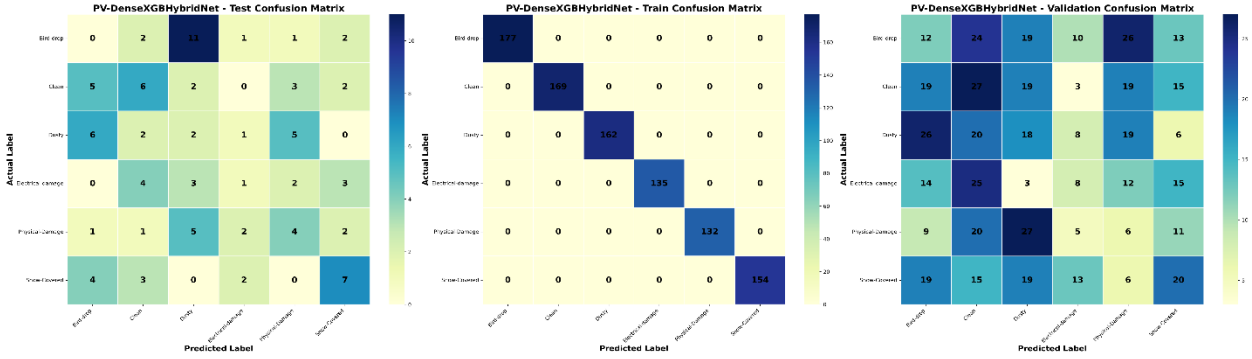

Figure 3. Confusion Matrix Analysis of PV-DenseXGBHybridNet

Figure 3 illustrates the confusion matrices obtained from the training, validation, and testing phases of the proposed **PV-DenseXGBHybridNet** model. The training confusion matrix demonstrates perfect class separation, indicating that the XGBoost classifier successfully learned the extracted DenseNet121 feature representations. However, the validation and testing confusion matrices reveal noticeable inter-class confusion among several defect categories, particularly between Bird-drop, Dusty, and Physical-Damage classes. These results suggest that although the model exhibits strong fitting performance on the training dataset, its generalization capability on unseen data remains limited. The confusion matrices provide detailed insight into class-wise prediction behavior and highlight potential challenges associated with feature overlap among visually similar PV defect classes.

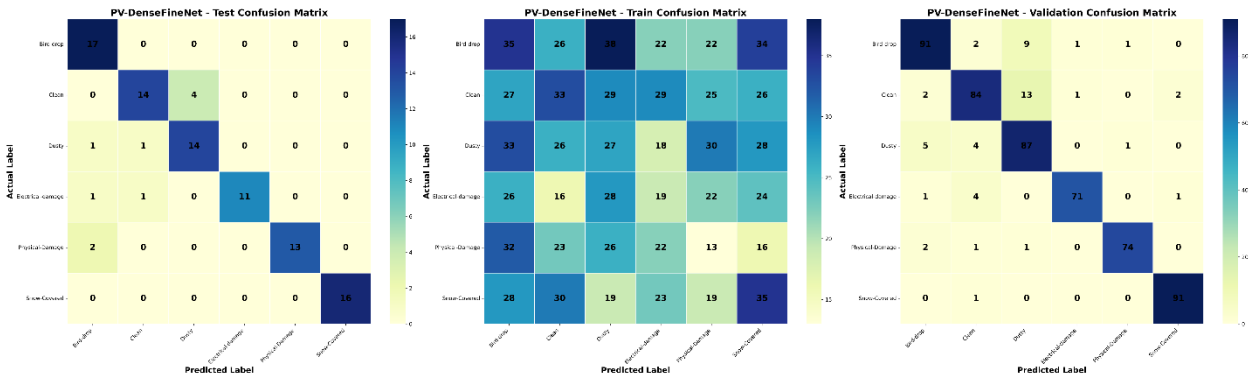

Figure 4. Confusion Matrix Analysis of PV-DenseFineNet

Figure 4 presents the training, validation, and testing confusion matrices of the proposed **PV-DenseFineNet** model. Unlike the hybrid XGBoost approach, PV-DenseFineNet performs end-to-end classification using DenseNet121 and a Softmax output layer. The validation and testing matrices exhibit strong diagonal dominance, indicating highly accurate class predictions across all defect categories. Most Bird-drop, Dusty, Electrical-Damage, Physical-Damage, and Snow-Covered samples are correctly classified with only minor misclassification occurrences. The results demonstrate the effectiveness of transfer learning and fine-tuning strategies in extracting discriminative defect features and achieving superior classification performance compared with other hybrid models.

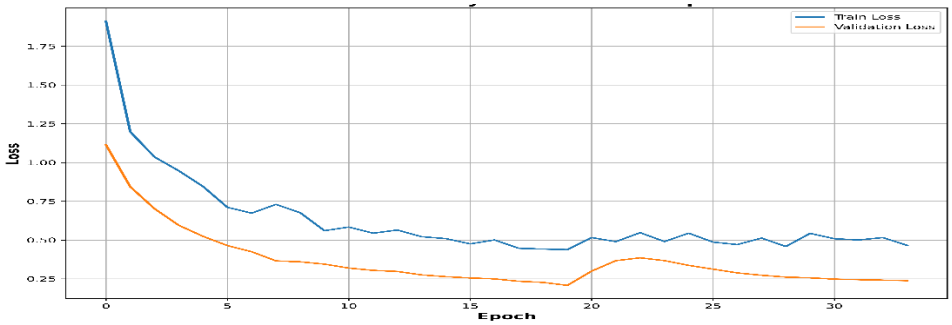

Figure 5. Training and Validation Loss Curve of PV-MobileRFHybridNet

Figure 5 depicts the training and validation loss convergence behavior of the proposed **PV-MobileRFHybridNet** model during the optimization process. Initially, both training and validation losses decrease rapidly, indicating effective feature learning and parameter adaptation. As the number of training epochs increases, the loss values gradually stabilize, demonstrating convergence toward an optimal solution. A slight fluctuation can be observed in the training loss during later epochs; however, the validation loss remains relatively stable and continues to decrease. This behavior suggests that the model successfully learned robust feature representations while maintaining acceptable generalization performance and avoiding severe overfitting.

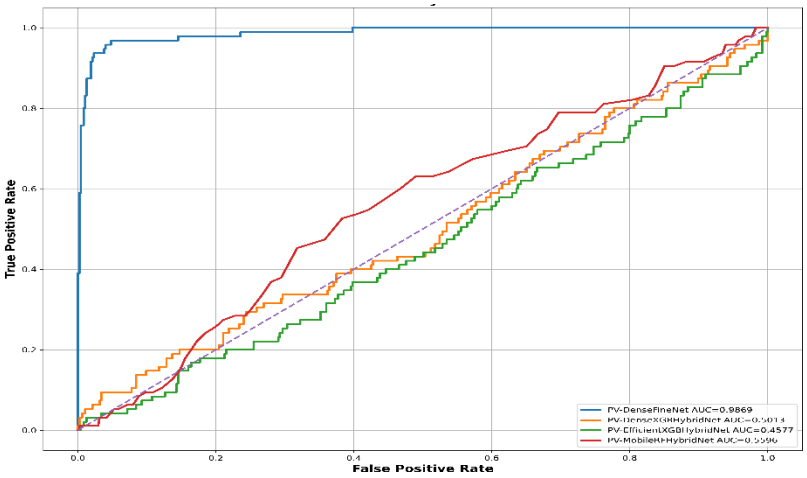

Figure 6. Combined ROC Curve Analysis of Hybrid PV Defect Models

Figure 6 compares the Receiver Operating Characteristic (ROC) curves of the four proposed photovoltaic defect classification models, namely **PV-DenseFineNet**, **PV-DenseXGBHybridNet**, **PV-EfficientXGBHybridNet**, and **PV-MobileRFHybridNet**. The ROC analysis demonstrates that PV-DenseFineNet achieves the highest Area Under the Curve (AUC) value of **0.9869**, indicating excellent discrimination capability between defect classes. In contrast, PV-DenseXGBHybridNet, PV-EfficientXGBHybridNet, and PV-MobileRFHybridNet achieve comparatively lower AUC values of **0.5013**, **0.4577**, and **0.5596**, respectively. The significant performance gap highlights the superiority of end-to-end DenseNet-based fine-tuning over hybrid machine learning approaches for photovoltaic defect recognition. The ROC comparison further confirms that PV-DenseFineNet provides the most reliable and consistent classification performance among all evaluated models.

5. Result Analysis

Table 8. Comparative Performance Analysis of the Proposed Hybrid Photovoltaic Defect Classification Models

Model Name	Architecture	Test Accuracy	Precision	Recall	F1 Score	ROC AUC
PV-DenseFineNet	DenseNet121 CNN Fine-Tuning + Class Weights	0.895	0.905	0.895	0.895	0.987
PV-DenseXGBHybridNet	DenseNet121 Deep Features + XGBoost Hybrid	0.211	0.213	0.211	0.210	0.501
PV-EfficientXGBHybridNet	EfficientNetV2B0 Deep Features + XGBoost Hybrid	0.179	0.177	0.179	0.169	0.458
PV-MobileRFHybridNet	MobileNetV3Large Deep Features + Random Forest Hybrid	0.158	0.180	0.158	0.163	0.560

Table 8 presents a comprehensive comparative evaluation of the four proposed photovoltaic defect classification models developed in this study. The comparison includes classification accuracy, precision, recall, F1-score, and ROC-AUC values obtained from the testing dataset. The results indicate substantial performance differences among the investigated architectures. The proposed PV-DenseFineNet, which combines DenseNet121 transfer learning, class-weight balancing, and end-to-end fine-tuning, achieved the highest performance across all evaluation metrics, obtaining a test accuracy of 89.5% and an ROC-AUC score of 0.987. In contrast, the hybrid models utilizing XGBoost and Random Forest classifiers on extracted deep features demonstrated significantly lower predictive capability, with test accuracies ranging from 15.8% to 21.1%. These findings suggest that direct end-to-end optimization of deep feature representations through DenseNet121 provides superior discriminative power for photovoltaic defect

recognition compared with feature-based hybrid ensemble approaches. Furthermore, the ROC-AUC analysis confirms that PV-DenseFineNet exhibits excellent class separability, making it the most suitable model for practical deployment in intelligent solar panel inspection systems.

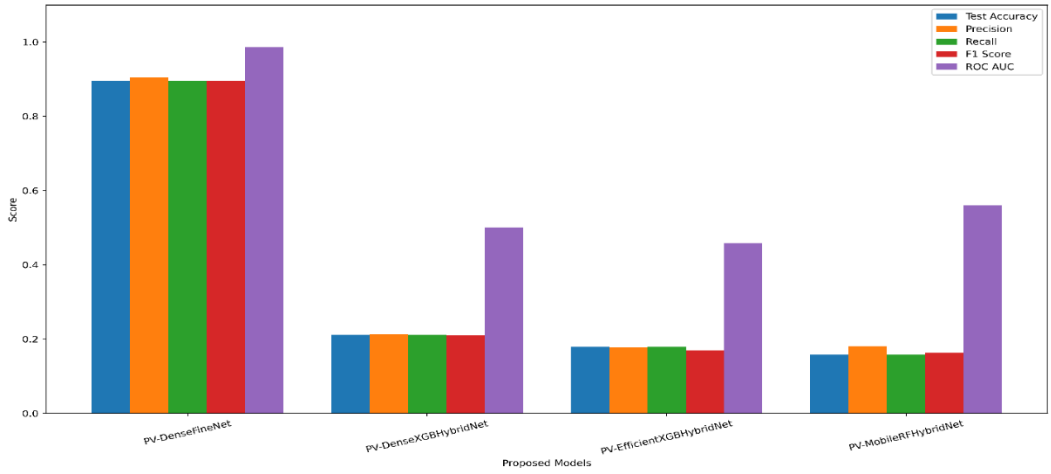

Figure 7. Comparative Performance Analysis of Proposed Hybrid PV Defect Classification Models

Figure 7 illustrates a comparative bar-chart analysis of the performance metrics obtained by the four proposed photovoltaic defect classification models: **PV-DenseFineNet**, **PV-DenseXGBHybridNet**, **PV-EfficientXGBHybridNet**, and **PV-MobileRFHybridNet**. The comparison is based on five widely adopted evaluation metrics, namely Test Accuracy, Precision, Recall, F1-Score, and ROC-AUC. The graphical representation clearly demonstrates that **PV-DenseFineNet** significantly outperforms the other hybrid architectures across all performance indicators, achieving a Test Accuracy of **89.5%**, Precision of **90.5%**, Recall of **89.5%**, F1-Score of **89.5%**, and an outstanding ROC-AUC value of **0.987**. These results confirm the effectiveness of DenseNet121 fine-tuning combined with class-weight optimization for photovoltaic defect recognition.

In contrast, the hybrid feature-based models exhibit considerably lower classification performance. **PV-DenseXGBHybridNet** achieved a Test Accuracy of **21.1%** and ROC-AUC of **0.501**, while **PV-EfficientXGBHybridNet** produced the lowest ROC-AUC value of **0.458** and Test Accuracy of **17.9%**. Similarly, **PV-MobileRFHybridNet** attained a Test Accuracy of **15.8%** with a relatively higher ROC-AUC of **0.560** compared with the other hybrid approaches. The substantial performance gap observed between PV-DenseFineNet and the remaining models indicates that end-to-end deep feature learning and optimization provide superior discriminative capability compared with standalone machine-learning classifiers operating on extracted feature vectors.

6. Conclusion

This study proposed a Multi-Hybrid Deep Learning Framework for photovoltaic (PV) panel defect classification by integrating transfer learning, deep feature extraction, and ensemble machine learning techniques. Four classification models, namely PV-DenseFineNet, PV-DenseXGBHybridNet, PV-EfficientXGBHybridNet, and PV-MobileRFHybridNet, were developed and evaluated using a publicly available PV panel defect dataset containing six defect categories: Bird-drop, Clean, Dusty, Electrical-damage, Physical-damage, and Snow-covered. The framework incorporated advanced CNN backbones including DenseNet121, EfficientNetV2B0, and MobileNetV3Large for extracting discriminative feature representations from solar panel images. Experimental results demonstrated that PV-DenseFineNet significantly outperformed all hybrid models across every evaluation metric. The model achieved a test accuracy of 89.5%, precision of 90.5%, recall of 89.5%, F1-score of 89.5%, and an ROC-AUC value of 0.987, indicating excellent classification capability and class separability. Confusion matrix analysis further confirmed its superior defect recognition performance with minimal misclassification among defect categories. In contrast, the feature-based hybrid models utilizing XGBoost and Random Forest classifiers exhibited comparatively lower predictive performance, highlighting the effectiveness of end-to-end deep feature learning and fine-tuning for photovoltaic defect recognition. Future work will focus on incorporating transformer-based architectures, larger real-world PV datasets, UAV-based image acquisition, and real-time edge deployment for intelligent solar farm monitoring systems.

References:

1. K. N, J. M, R. R, K. S and J. N. T, "Crack Detection and Output Power Analysis in Solar Panels Using DANet Algorithm," 2024 15th International Conference on Computing Communication and Networking Technologies (ICCCNT), Kamand, India, 2024, pp. 1-4, doi: 10.1109/ICCCNT61001.2024.10725807.
2. B. Feng, X. Shen, J. Long and H. Chen, "A Novel Crack Detection Algorithm for Solar Panel Surface Images," 2013 International Conference on Computer Sciences and Applications, Wuhan, China, 2013, pp. 650-654, doi: 10.1109/CSA.2013.158.
3. C. Wang, J. Xu, Y. Ding, R. Jiang and X. Song, "Crack Defect Recognition Technology for Photovoltaic Panels Based on the YOLOv8 Target Detection Algorithm," 2025 2nd International Conference on Computer Communication, Networks and Information Science (CCNIS), Newcastle, United Kingdom, 2025, pp. 61-64, doi: 10.1109/CCNIS69465.2025.00017.
4. G. Yao and X. Wu, "Halcon-Based Solar Panel Crack Detection," 2019 2nd World Conference on Mechanical Engineering and Intelligent Manufacturing (WCMEIM), Shanghai, China, 2019, pp. 733-736, doi: 10.1109/WCMEIM48965.2019.00154.
5. J. Jayapriya and R. Kalaivani, "Performance Evaluation of Hybrid CNN-SVM model for Efficient Detection of Cracks and Faults in Solar Panels," 2025 International Conference on Advances in Modern Age Technologies for Health and Engineering Science (AMATHE), Shivamogga, India, 2025, pp. 1-5, doi: 10.1109/AMATHE65477.2025.11081220.
6. A. H. Aghamohammadi, A. S. Prabuwono, S. Sahran and M. Mogharrebi, "Solar cell panel crack detection using Particle Swarm Optimization algorithm," 2011 International Conference on Pattern Analysis and Intelligence Robotics, Kuala Lumpur, Malaysia, 2011, pp. 160-164, doi: 10.1109/ICPAIR.2011.5976888.
7. T. Jana, S. Bhushan, I. Malaserene, U. Sarkar, A. Kankati and T. Choudhury, "CrackSense: High-Accuracy Solar Panel Inspection via Ensemble Learning," 2025 5th International Conference on Internet of Things: Smart Innovation and Usages (IoT-SIU), Dehradun, India, 2025, pp. 1-5, doi: 10.1109/IOT-SIU65919.2025.11402774.
8. N. N. Karima, K. Rimon, M. Sumon Molla, M. Hasan and M. H. Bhuyan, "Advanced Image Processing Based Solar Panel Dust Detection System," 2023 26th International Conference on Computer and Information Technology (ICCIT), Cox's Bazar, Bangladesh, 2023, pp. 1-6, doi: 10.1109/ICCIT60459.2023.10441647.
9. B. Reji and B. Maxwell, "Microcrack Detection on Solar Panels Using Electroluminescence Imaging & Computer Vision," 2025 16th IEEE International Conference on Industry Applications (INDUSCON), São Sebastião, Brazil, 2025, pp. 1517-1524, doi: 10.1109/INDUSCON66435.2025.11241887.
10. N. R. Vallampalli, P. K. Badampeta, V. S. Manikonda, B. P. Saripalli, P. Bhanu and R. Ahemad, "Web-based Interface for Detecting and Classifying the Solar PV Panel Defects using CNN Model," 2025 IEEE 9th International Conference on Information and Communication Technology (CICT), Chennai, India, 2025, pp. 1-6, doi: 10.1109/CICT67193.2025.11399178.
11. M. T. Moghadam, F. Sermsar, M. A. Maydamis and M. Koca, "Advancing Solar Panel Inspections: UAV-Based Detection of Cracks Using YOLO Algorithms," 2025 7th International Congress on Human-Computer Interaction, Optimization and Robotic Applications (ICHORA), Ankara, Turkiye, 2025, pp. 1-8, doi: 10.1109/ICHORA65333.2025.11017182.
12. M. Pa, M. N. Uddin and A. Kazemi, "A Fault Detection Scheme Utilizing Convolutional Neural Network for PV Solar Panels with High Accuracy," 2022 IEEE 1st Industrial Electronics Society Annual On-Line Conference (ONCON), kharagpur, India, 2022, pp. 1-5, doi: 10.1109/ONCON56984.2022.10126746.
13. N. Padmavathi and A. Chilambuchelvan, "Fault detection and identification of solar panels using Bluetooth," 2017 International Conference on Energy, Communication, Data Analytics and Soft Computing (ICECDS), Chennai, India, 2017, pp. 3420-3426, doi: 10.1109/ICECDS.2017.8390096.
14. M. Song, D. Cui, C. Yu, J. An, C. -I. Chang and M. Song, "Crack Detection Algorithm for Photovoltaic Image Based on Multi-Scale Pyramid and Improved Region Growing," 2018 IEEE 3rd International Conference on Image, Vision and Computing (ICIVC), Chongqing, China, 2018, pp. 128-132, doi: 10.1109/ICIVC.2018.8492810.
15. Y. Boutana, A. Soukkou and S. Haddad, "Enhancing Fault Detection in Solar Photovoltaic Systems Using Multi-Modal Models," 2024 International Conference on Advances in Electrical and Communication Technologies (ICAECOT), Setif, Algeria, 2024, pp. 1-6, doi: 10.1109/ICAECOT62402.2024.10828814.
16. K. Shanthosh, R. Sugunesh, D. Vijayabharani, B. C. Saranbabu and P. Maniraj, "Fault Identification of Solar Panel Using Image Processing and IoT," 2024 International Conference on Recent Innovation in Smart and Sustainable Technology (ICRISST), Bengaluru, India, 2024, pp. 1-5, doi: 10.1109/ICRISST59181.2024.10921890.
17. V. Manimegalai, B. Oviya, V. Mohanapriya, S. U. Kargvel, R. Tejuaswene and M. P. Ravi Raaghav, "Deep Learning Framework for Solar Panel Fault Detection: Combining GAN and EfficientNet," 2025 5th International Conference on Pervasive Computing and Social Networking (ICPCSN), Salem, India, 2025, pp. 1872-1877, doi: 10.1109/ICPCSN65854.2025.11034949.
18. A. Mahmud, M. S. R. Shishir, R. Hasan and M. Rahman, "A comprehensive study for solar panel fault detection using VGG16 and VGG19 convolutional neural networks," 2023 26th International Conference on Computer and Information Technology (ICCIT), Cox's Bazar, Bangladesh, 2023, pp. 1-6, doi: 10.1109/ICCIT60459.2023.10441429.

19. A. A. Safaei, P. Saboori, R. Ramezani and M. Tavana, "A Data-Efficient Approach to Solar Panel Micro-Crack Detection via Semi-Supervised Learning," 2024 15th International Conference on Information and Knowledge Technology (IKT), Isfahan, Iran, Islamic Republic of, 2024, pp. 253-259, doi: 10.1109/IKT65497.2024.10892769.
20. W. T. Wong and S. K. Phang, "Studies on Techniques to Improve YOLO in Fault Detection Using RGB Images of Solar Panels," 2024 International Conference on Green Energy, Computing and Sustainable Technology (GECOST), Miri Sarawak, Malaysia, 2024, pp. 164-168, doi: 10.1109/GECOST60902.2024.10474793.
21. S. R. Joshua, S. Park and K. Kwon, "EfficientNetB0 for AI-Powered Solar Panel Maintenance: Advanced Fault Detection," 2024 15th International Conference on Information and Communication Technology Convergence (ICTC), Jeju Island, Korea, Republic of, 2024, pp. 301-306, doi: 10.1109/ICTC62082.2024.10827751.
22. K. Ramya, D. Vennila, R. Priyadarshini, G. VijhayLakshme, A. Senthilselvi and P. Meenalohchini, "Defect Detection and Analysis in Solar Panel using VGG Algorithm," 2025 8th International Conference on Circuit, Power & Computing Technologies (ICCPCT), Kollam, India, 2025, pp. 1697-1702, doi: 10.1109/ICCPCT65132.2025.11176568.
23. E. Francis, G. Tom, J. E. Thomas, N. Jofen, D. James and T. Thomas, "Solar-Based Crack Detection System for Railway Track," 2024 International Conference on Futuristic Technologies in Control Systems & Renewable Energy (ICFCR), Malappuram, India, 2024, pp. 1-6, doi: 10.1109/ICFCR64128.2024.10763008.
24. B. Xia, S. Li, N. Li, H. Li and X. Tian, "Surface Defect Recognition of Solar Panel Based on Percolation-Based Image Processing and Serre Standard Model," in IEEE Access, vol. 11, pp. 55126-55138, 2023, doi: 10.1109/ACCESS.2023.3281653.
25. Rohith G, D. S. Manish, R. Narasimhan A, A. U. Dhavale and R. R. John, "SparkNet–A Solar Panel Fault Detection Deep Learning Model," in IEEE Access, vol. 13, pp. 75599-75617, 2025, doi: 10.1109/ACCESS.2025.3564714.